Available online at www.sciencedirect.com

ScienceDirect

Physics Procedia 74 (2015) 340 – 346

Physics Procedia

Conference of Fundamental Research and Particle Physics, 18-20 February 2015, Moscow, Russian Federation

The distribution of neutron absorbing time in the neutron detector of the GAMMA-400 space observatory

I.I. Gnezdilov[a]*, V.I. Mukhin[a], M.A. Demichev[b]

[a]*National Research Nuclear University MEPhI (Moscow Engineering Physics Institute),Kashirskoe Shosse 31, Moscow 115409, Russia*
[b]*Joint Institute for Nuclear Research (JINR), Joliot-Curie 6, Dubna 141980, Moscow region, Russia*

Abstract

The neutron detectors (ND) have been designed for the future GAMMA-400 space observatory with ^{3}He-counters and ^{6}LiF/ZnS(Ag) scintillation screens. The ND contribution in the rejection factor for protons in the GAMMA-400 is considered with significantly different number of neutrons generated in the electromagnetic and hadronic cascades. The ND is predominantly made from polyethylene, it has sizes of 100×100×10 cm^3. GEANT4 simulation was obtained by the differential distribution of neutron absorbing time as the function of the registration time for different ^{3}He, ^{6}Li concentration. Nomograms were constructed for determining neutrons miscount depending on the number of neutrons crossing the ND and time resolution of the ND. The simulation results showed that the ND with 33 ^{3}He-counters detected the neutron fluence 0.23 n/cm^2 without neutrons miscount.

Peer-review under responsibility of the National Research Nuclear University MEPhI (Moscow Engineering Physics Institute)

Keywords: electron burst; radiation belt; robust regression;absorbing time

1. Introduction

Currently in the field of astrophysics, the following are actual scientific goals: study of the origin of the dark matter by means of gamma-ray astronomy; precise measurements of Galactic and extragalactic discrete astrophysical sources; research of high-energy gamma-ray bursts; research of high-energy electron + positron fluxes; research of high-energy nuclei fluxes. To solve these problems is the GAMMA-400 space observatory (GAMMA-400).

* Corresponding author. Tel.: +7-495-788-5699.
E-mail address: y.gnezdilov@gmail.com

Peer-review under responsibility of the National Research Nuclear University MEPhI (Moscow Engineering Physics Institute)
doi:10.1016/j.phpro.2015.09.188

It is optimized for the energy 100 GeV and is able to measure gamma-ray and electron + positron fluxes in the energy range from 100 MeV – 3000 GeV. GAMMA-400 contains two calorimeters CC1 and CC2 with total thickness $25X_0$. Both CC1 and CC2 consists of CsI(Tl) crystals. The GAMMA-400 contains the neutron detector (ND) placed just under the calorimeter [1]. The size of the ND is 100×100×10 cm^3. The ND contribution in the rejection factor for protons in the GAMMA-400 is considered with significantly different number of neutrons generated in the electromagnetic and hadronic cascades. To estimate the number of neutrons produced in the shower, it was used well-known results of computer modeling of showers in the calorimeter using GEANT4. The efficiency of neutron detection and timing resolution of the ND is not taken into account in the present simulation [2].

The idea of enhancing calorimeter discrimination by measuring the neutron component of the showers, was first tried with the PAMELA experiment on satellite [3]. Two devices of the PAMELA spectrometer were used in the experiment: the calorimeter and the ND [4]. The calorimeter is composed of layers of tungsten absorber and silicon detectors planes. The total depth is about 16:3 radiation lengths and about 0:6 interaction length. The neutron detector is placed under the calorimeter. It contains 36 ^{3}He-counters surrounded by the polyethylene moderator ~ 9 cm thick. The calorimeter was exposed to a beam of electrons and protons with energy in the range of 20–180 GeV. When a high-energy hadron interacts inside the calorimeter, the neutrons from the decay of excited nucleus are produced. Afterward, a part of these neutrons is thermalized by the polyethylene moderator and recorded by the ^{3}He-counters. After the acquisition system of the PAMELA spectrometer was triggered the ND recorded the number of neutrons during 200 μs, the time needed for majority of neutrons to be thermalized.

In article [5] studied the neutron component of the showers in the electromagnetic calorimeter CALET, which consists of consists of BGO crystals (60 cm × 60 cm × 30 cm height). For each simulated event the produced neutrons have been propagated till they reached the outside of the calorimeter. The energy, direction and arrival time of each neutron exiting the calorimeter from the bottom side where the ND is placed. The rejection factor achievable for hadronic showers can be as high as ~ 10^3 just considering the neutron counting.

Average numbers of neutrons generated in the electromagnetic and hadronic cascades in the mentioned calorimeters are shown in Table 1.

Table 1. Average numbers of neutrons (n) generated in the electromagnetic and hadronic cascades in the various calorimeters.

Calorimeters	Area of the input surface, cm^2	E_e, GeV	n	E_p, GeV	n
GAMMA-400 [2]	100×100	100	30	*)	350
PAMELA [4]	60×60	180	0.6	150	2.7
CALET [5]	60×60	400	20	1000	670

*) E_p> 100 GeV (the proton energy spectral index is equal to -2.7)

As can be seen, the interaction of primary electrons and primary protons from the calorimeter produces a small amount of evaporated neutrons with an average energy of about ~ 2 MeV. At the same time, the neutron yield of the calorimeter and passing through the detector for a short time, constituting 10–100 ns after the shower core. Next neutrons fall into the moderator, heat and are registered. To successfully use ND for rejection of electronic and hadron showers not only high efficiency detection of neutrons is required, but also high time resolution to exclude neutrons miscount.

2. GEANT4 simulation

GEANT4 software toolkit is used for simulation and Monte Carlo calculation of neutron absorption efficiency of the ND and the differential distribution of neutron absorbing time. Energy spectrum of the outgoing evaporated neutrons could be simulated by ^{252}Cf source spectrum with average neutron energy of ~ 2.2 MeV.

Outgoing of the calorimeter neutrons cross ND and slowed to thermal energy in the moderator. Neutrons are detected by the following neutron reaction:

$$n + {}^3He \rightarrow p + {}^3H + 0.76\ MeV, \text{ cross section } \sigma(E_n = 0.025) = 5330 \text{ barn for } {}^3\text{He} \quad (1)$$

$$n + {}^6Li \rightarrow \alpha + {}^3H + 4.78\ MeV, \text{ cross section } \sigma(E_n = 0.025) = 940 \text{ barn for } {}^6\text{Li} \quad (2)$$

Neutron absorption efficiency is defined as the number of protons or alpha-particles that appear in reaction (1) or (2) divided by the number of neutrons outgoing from the calorimeter and crossing the ND. Each absorbed neutron is supposed to give an impulse which is registered.

During the interaction of primary electrons and primary protons with the calorimeter a shower of charged particles is created which make a background. In order to reduce the contribution of background events, the simulation was performed after 400 ns a neutron crossed the ND (the number of incident neutrons was 10^6 neutrons).

2.1. The design of the ND for GAMMA-400

As shown in Fig. 1(a), the ND for GAMMA-400 consists of successive moderator layers, ^{3}He-counters (d = 30 mm, L = 100 cm) and a neutron reflector. The moderator and the neutron reflector layers are 3 cm and 4 cm in thickness respectively and both consist of high-density polyethylene. Optimal thicknesses were chosen by numerical simulation method. The ND contains 33 ^{3}He-counters. The commercial ^{3}He-counter type Helium-30/1020 is used. It is manufactured by SPF "CONSENSUS" (http://consensus-group.ru/). The time resolution of a single ^{3}He-counter in a proportional mode is ~ 2 μs and the time resolution of the ND is ~ 0.1 μs, because it contains 33 independent registration channels.

As shown in Fig. 1(b), another version of the ND for GAMMA-400 consists of successive layers: moderator, upper scintillation screen, first light guide, middle scintillation screen, second light guide, lower scintillation screen and neutron reflector. There were used commercial scintillation screens based on ^{6}LiF/ZnS(Ag), manufactured Eljen Technology and Applied Scintillation Technologies (now the new name Scintacor). Scintillation screens are in optical contact with two layers of the light guides which are made of wavelength shifting plastics at the size of 100×10×1.5 cm^3 band form. There are 10 light intercepting bands in each layer. The decay time of the prompt scintillation component is 0.2 μs. The time resolution of the ND with scintillation screens is ~ 0.02 μs, because it contains 10 independent registration channels.

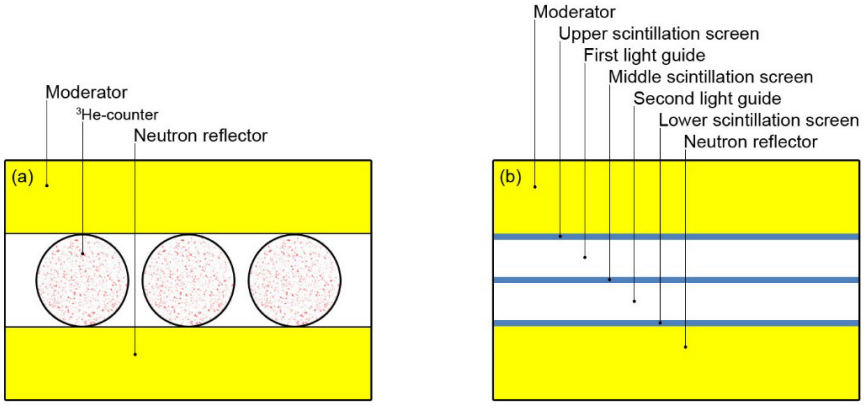

Fig. 1. The ND for GAMMA-400 design: (a) with ^{3}He-counters, (b) with scintillation screens.

There were performed calculations using ^{3}He-counters with various pressure and scintillation screens with different ^{6}Li concentration. ^{3}He and ^{6}Li concentrations are shown in Table 2 and Table 3 respectively.

Table 2. ^{3}He concentration in the ND by weight.

The pressure of the gas mixture in ^{3}He-counter, atm.	^{3}He concentration in the ND by weight, %
3	0.017
6	0.034
9	0.052

Table 3. ^{6}Li concentration in the ND by weight.

ND with three scintillation screens 100×100 cm^2.	^{6}Li concentration in the ND by weight, %
AST	0.067
AST2	0.121
EJ-426HD	0.153
EJ-426HD2	0.239

2.2. Scintillation screen

The use of ^{6}LiF/ZnS(Ag) scintillation screens in the ND construction for the GAMMA-400 was proposed for the first time in the article [6]. The ^{6}LiF / ZnS (Ag) phosphor is a mechanical mixture of dispersed scintillator ZnS(Ag) with ^{6}LiF enriched by ^{6}Li. The scintillation screen is formed by the dispersion of the phosphor into a colorless binder (acrylic resin). Properties of commercial scintillation screens are shown in Table 4.

Table 4. Properties of a commercial scintillation screens.

Type scintillation screens*)	^{6}LiF:ZnS mix ration by weight	^{6}Li isotope estimated atomic volume density, atoms/cc x10^{21}	Thickness, mm	Estimated thermal neutron capture efficiency, %
AST	1:2	12.9	0.25	26
AST2	1:4	7.77	0.45	28
EJ-426HD	1:2	13.9	0.32	34
EJ-426HD2	1:2	13.9	0.50	48

3. Results

In Fig. 3 and Fig. 4, there is shown the differential distribution of absorbing time of neutrons (after 400 ns) for the period from 400 ns to 200 μs with an integration time of 1 μs. The function is normalized as if the front surface of the ND crossed by 5000 neutrons with the spectrum of ^{252}Cf. The results obtained on the assumption that 5000 neutrons are uniformly distributed over the front surface of the ND with the area of 100×100 cm^2, i.e. the neutron fluence is 0.5 n/cm^2. The calculated error in determining the differential distribution of absorbing time of neutrons on Fig. 3 and Fig. 4 is about 5%.

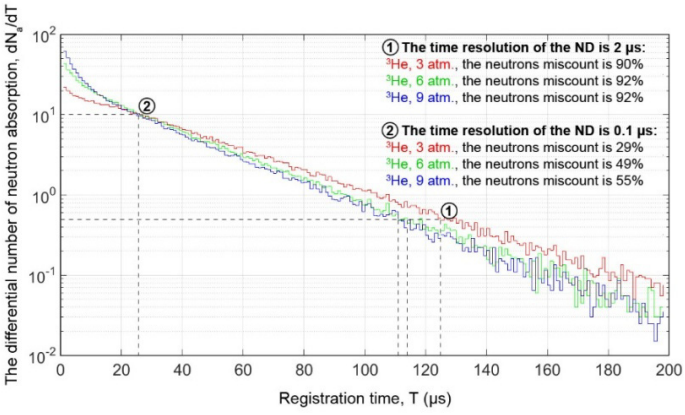

Fig. 2. The differential distribution of neutron absorbing time (after 400 ns) with an integration time of 1 μsfor 5000 neutrons that crossed the ND with ^{3}He-counters.

The time resolution of a single ^{3}He-counter (2 μs) is deficient for the efficient detection of 5000 neutrons. The neutrons miscount is ~ 90%. At the same time, the time resolution of the ND with ^{3}He-counters (0.1 μs) reduces the number of miscounted neutrons by 3 times.

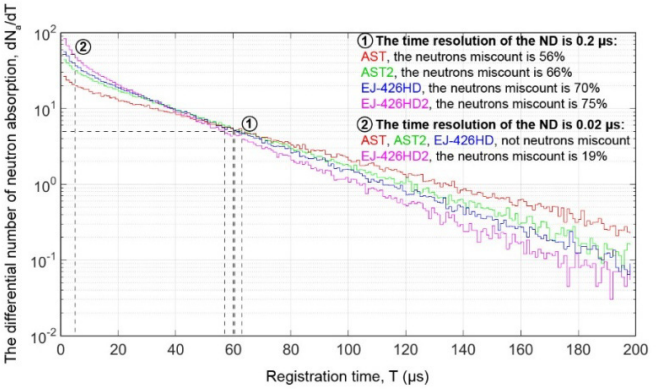

Fig. 3. The differential distribution of neutron absorbing time (after 400 ns) with the integration time of 1 μs for 5000 neutrons that crossed the ND with scintillation screens.

The time resolution of a scintillation screen (0.2 μs) is deficiency for the efficient detection 5000 neutrons. The neutrons miscount is ~ 70%. At the same time, the time resolution of the ND with scintillation screens (0.02 μs) is registered without neutrons miscount. However the ND with a ^{6}Li concentration of 0.239% by weight so greatly reduces the lifetime of neutrons from entering into the ND until absorption that registration with the neutrons miscount is ~ 20%.

4. Discussion

Fig. 4 and Fig. 5 show nomograms – the neutrons miscount as a function of producing the number of neutrons crossing the ND with ^{3}He-counters and the ND with scintillation screens with the time resolution of the ND. Nomograms are obtained on the basis of differential distribution of absorbing time of neutrons, which are represented in Fig. 2 and Fig. 3. The experimental values (the points on nomograms) are fitting the function: $f(x) = a \times x^b + c$, wherein the adjusted R-square is ~ 0.997.

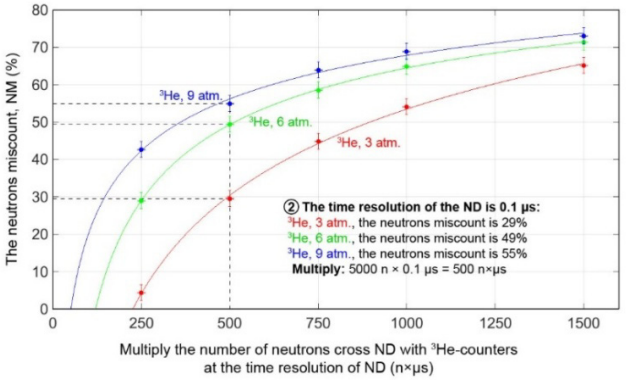

Fig. 4. The neutrons miscount as a function of producing the number of neutrons that crossed the ND with ^{3}He-counters at the time resolution of ND (the function of fitting: $f(x) = a \times x^b + c$).

For a given time resolution (0.1 μs) for the ND with ^{3}He-counters (3 atm.), there is defined the registration time interval of $T = 25$ μs (Fig. 2), after which the number of absorbed neutrons becomes smaller the number of detected neutrons. During this period ($T = 25$ μs) the number of absorbed neutrons ($N_a = 354$) and a number of neutrons that can be detected ($N_d = 250$) are calculated. The neutrons miscount (NM) is ~ 29% (Fig. 4):

$$NM = (N_a - N_d) / N = (354 - 250) / 354 = 0.294, \quad (3)$$

The obtained neutrons miscount corresponds to the neutron fluence of 0.5 n/cm^2. Thus, producing the number of 5000 neutrons that cross the ND with ^{3}He-counters (3 atm.) at the time resolution (0.1 μs) is 500 n×μs (Fig. 4).

As can be seen from the data shown in Fig. 4, the least neutrons miscount is achieved in the ND with ^{3}He-counter with the pressure of 3 atm. For the ND with ^{3}He-counters with the pressure of 3 atm., 6 atm., 9 atm. and time resolution of ~ 0.1 μs NM = 0, when the total number of neutrons crossing the ND is: 2270, 1210, 510 (Fig. 4). Thus, the ND with ^{3}He-counters with the pressure of 3 atm. allows to detect the neutron fluence 0.23 n/cm^2 without neutrons miscount.

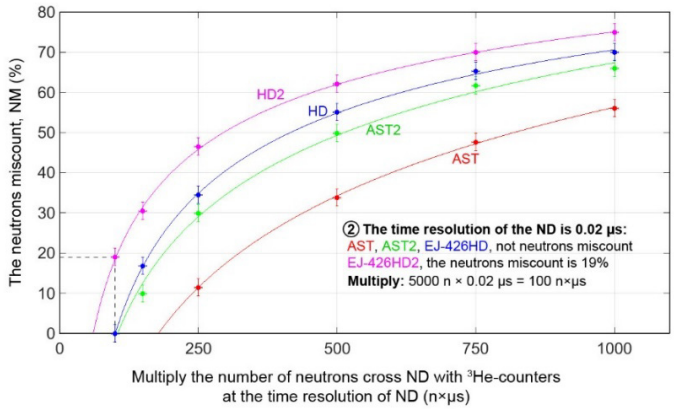

Fig. 5. The neutrons miscount as a function of producing the number of neutrons crossing the ND with scintillation screens at the time resolution of the ND (the function of fitting: $f(x) = a \times x^b + c$).

The neutrons miscount of the ND with scintillation screens increases with the ^{6}Li concentration as well as the neutrons miscount of the ND with ^{3}He-counters with increasing ^{3}He concentration (Fig. 5). For the ND with scintillation screens (AST, AST2, EJ-426HD, EJ-426HD2) and the time resolution of ~ 0.02 μs NM = 0, when the total number of neutrons crossing the ND is: 8950, 5250, 5000, 3050. Thus, the ND with scintillation screen (AST) detects the neutron fluence 0.9 n/cm^2 without neutrons miscount.

5. Conclusions

The neutron detector with ^{3}He-counters may be the same as in the PAMELA. When using 33 ^{3}He-counters (d = 30 mm, L = 100 cm, pressure 3 atm.) the ND detects the neutron fluence until 0.3 n/cm^2 without the neutrons miscount. Such neutron fluence may be when electromagnetic calorimeter of a proton interacts with the energy of a few TeV.

Despite the fact that the time resolution of the ND with scintillation screens is 10 times higher than that of the one with ^{3}He-counters, the ND with scintillation screens allows to detect the neutron fluence ~ 4 times higher without the neutrons miscount and this construction will be used in GAMMA-400 space observatory.

Acknowledgements

The authors acknowledge Irina Popova for the creating conditions for the article writing and Azat Fattakhov in its assistance. The work is done at their own expense authors.

References

[1] Galper A.M., Adriani O., Aptekar R.L. *et al.* Characteristics of the GAMMA400 Gamma-Ray Telescope for Searching for Dark Matter Signatures. *Bulletin of the Russian Academy of Sciences. Physics* 2013;77(11):1339–1342.
[2] Leonov A.A., Galper A.M., Bonvicini V. *et al.* A separation of electrons and protons in the GAMMA-400 gamma-ray telescope. arXiv:1503.06657v1 [astro-ph.IM] 2015.
[3] Picozza P., Galper A.M., Castellini G. *et al.* PAMELA – A payload for antimatter matter exploration and light-nuclei astrophysics. *Astropart. Phys.* 2007;27:296-315.
[4] Stozhkov Y.I., Basili A., Bencardino R. *et al.* About separation of hadron and electromagnetic cascades in the PAMELA calorimeter. *International Journal of Modern Physics A* 2005;20(29):6745–6748.
[5] Adriani O., Bonechi L., Bongi M. *et al.* Enhancement of hadron–electron discrimination in calorimeters by detection of the neutron component. *Nucl. Instrum. and Methods in Physics Research A* 2011;628:332–338.
[6] Mukhin V.I. Polycrystalline scintillator neutron detector. 3d International Conference on Engineering of Scintillation Materials and Radiation Technology ISMART-2012, Dubna, 2012;59–60.